CHAPTER 2

Theoretical Background

CHAPTER – 2

THEORETICAL BACKGROUND

2.1 THEORY OF MÖSSBAUER SPECTROSCOPY:

2.11 INTRODUCTION:

Mössbauer spectroscopy is a well known and most versatile technique. It is used to study some weak interactions between the nucleus and the surroundings. Mössbauer effect has found applications in various fields in science such as nuclear physics, solid state physics, chemistry, relativity, biology and geology. Mössbauer effect is an accidental observed phenomenon which was observed by R. L. Mössbauer in 1957.

Mössbauer spectroscopy, a nuclear resonance technique is based upon an effect known as the 'Mössbauer effect' after the name of its discoverer R. L. Mössbauer[1]. For this effect, which is often defined as the recoilless emission and resonant absorption of gamma rays by nuclei bound in solid, he was awarded Nobel prize in 1961. Mössbauer effect can be reworded as gamma ray resonance fluorescence. Prior to Mössbauer's work it was difficult to detect the sum of the recoil energies given to the emitting and absorber nuclei (subtracted from the emitted gamma ray energy) in order to conserve momentum was large to destroy resonant absorption. Also, thermal motions broadened the spectra and reduced the absorption cross-section at resonance. Mössbauer found the resonance fluorescence increased with increasing temperature. He explained his result by recognising that when the source is cooled, an increased fraction of gamma rays is emitted for which the recoil momentum is given to the entire crystal lattice and not to a single nucleus. The crystal being much massive than nucleus, suffers negligible recoil in absorbing the recoil momentum. Thus this process is called recoilless emission.

Similarly a recoilless absorption may take place when the absorbing nuclei are bound in solid.

2.12 MÖSSBAUER EFFECT:

When the nuclei of atoms, bound in a crystal lattice, can absorb or emit γ-ray photons without the loss of energy due to recoil and Doppler broadening . This phenomenon is known as Mössbauer effect. Mössbauer effect is also known as recoilless gamma resonance fluorescence. The recoilless emission or absorption of gamma ray is provided by embedding a crystal or source in a crystal lattice. Emitted gamma ray gives up their momentum to the nucleus and then the momentum is distributed over the crystal by lattice forces in all direction and gives rise to a recoilless emission of gamma rays. Similarly, during the absorption of gamma ray, nucleus receives the momentum from the absorbed gamma ray and then momentum is distributed all over the crystal and resonance absorption becomes recoilless. The condition to observe the resonance fluorescence absorption is that the sum of the recoil energies given to the emitting or absorbing nuclei should be small enough. In general, a system emits a photon while making a transition from one state to another of lower energy. If the photon has just the right energy to cause a transition to the higher energy state, the reverse process can takes place and this process is called resonant absorption. The fraction of recoilless absorption or emission of gamma ray is given by

$$E_R = (1-f)h\omega$$

Where E_R is the energy of recoil gamma ray. The probability of zero phonon emission or absorption for a Mössbauer isotope embedded in a lattice can be calculated quantitatively [1].

Assuming a Gaussian distribution for the atom with a mean square vibrational amplitude of the emitting atom $\langle x^2 \rangle$ in the direction of γ-ray wave

vector k, the probability for recoilless emission is

$$f = \exp\left[-\frac{4\pi\langle x^2\rangle_T}{\lambda^2}\right] \qquad (1)$$

Here the fraction of events 'f' is the factor which makes the Mössbauer effect observable.

For a solid, $K_B\theta_D$ may be used as the typical phonon energy, θ_D is the Debye temperature of the solid and K_B is the Boltzmann constant. If $E_R < K_B\theta_D$ then only few γ-rays will produce the phonon excitations and a good fraction of γ-rays will result in zero phonon transition. As the temperature increases more and more phonon will be excited in the lattice and zero phonon emission decreases.

Equation 1 can be also written as[2-3]

$$f = \exp\left[-\frac{4\pi\langle x^2\rangle_T}{\lambda^2}\right] \qquad (2)$$

where $\langle x^2\rangle_T$ is the mean square amplitude of the absorbing or emitting nuclei.

The above Equation 2 can also be written in terms of Debye temperature θ_T of the solid,

$$f = \exp\left[\left(\frac{-6E_R}{k\theta_D}\right)\left\{\frac{1}{4}+\left(\frac{T}{\theta_D}\right)^2\int_0^{\theta_D/T}\left(\frac{x}{e^x-1}\right)dx\right\}\right] \qquad (3)$$

In Equation 2 $\langle x^2\rangle_T/\lambda^2$ is a factor governing the condition for Mössbauer effect. The above Equation 3 is often written as

$$f = \exp(-2W) \qquad (4)$$

Where factor W is called Lamb-Mössbauer factor for Debye-Waller factor[3] At low temperature, $T<<\theta_D$, θ_D/T can be replaced by ∞ and the recoil free fraction reduces to

$$f = \exp\left[-\frac{3}{2}\frac{E_R}{k\theta_D}\left(1+\frac{2}{3}\frac{\pi^2 T^2}{\theta_D^2}\right)\right] \qquad (5)$$

for $T \geq \theta_D/2$

$$f = \exp\left[-\frac{6 E_R T}{k \theta_D^2}\right] \qquad (6)$$

From the above equation it is evident that the probability of observing Mössbauer effect increases with

(i) decreasing recoil energy i.e. decreasing transition energy.

(ii) decreasing temperature

(iii) increasing Debye temperature θ_D.

2.13 Fe^{57} AS A MÖSSBAUER PROBE IN A MÖSSBAUER SPECTROSCPY:

In all radioactive sources Fe^{57} is a most common and suitable source for Mössbauer spectroscopy. The conditions for observation of Mössbauer spectroscopy are as follows.

(a) In resonance absorption, the transition must be ground state.

(b) Smaller value of gamma ray energy $E\gamma$ and recoil energy E_R .

(c) Sufficiently long life time of a radioactive isotope to collect a large number of data.

(d) Suitable magnitude of nuclear state life time to get a narrow line width for observing a smaller energy changes.

(e) Larger value of absorption cross-section.

Presently Mössbauer spectroscopic measurements have been made with about 103 transitions of 44 different elements[4].

In a Mössbauer spectroscopy most of the measurements were done with transition from I=(3/2)$^-$ to (1/2)$^-$ of 14.4 keV gamma ray in Fe^{57} (Figure 2.11). Fe^{57} have a following advantages over other sources.

$^{57}_{26}Fe$(14.4keV,136.5keV)

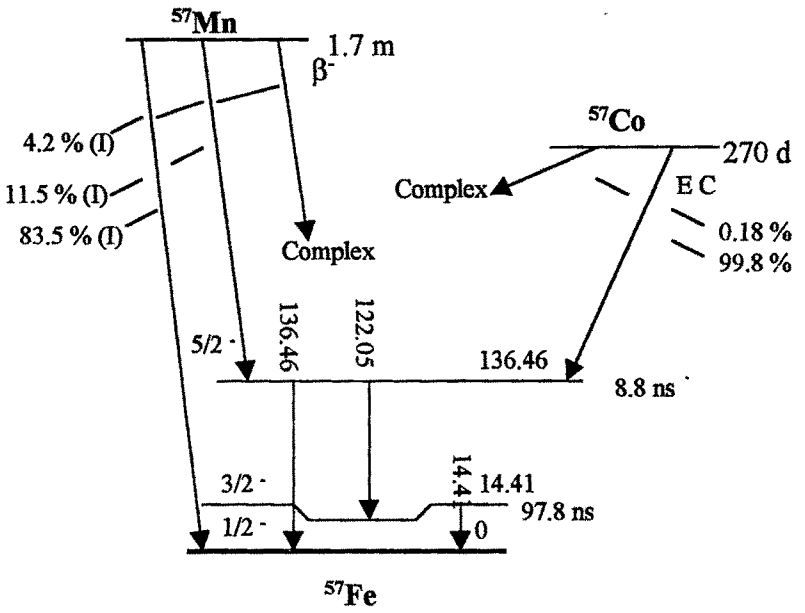

Measurement Properties (E_γ= 14.4 keV)

E_γ= 14.4125 ± 0.0006 keV
$t_{1/2}(\gamma M)$ =97.81 ± 0.14 ns)
$\alpha_T(\gamma M)$ =8.18 ± 0.16
IA = 2.19 %
MG = + 0.0904206 ± 0.0000012 nm
MM = - 0.15491± 0.00023 nm
QM = +0.187 ± 0.005 b

Measurement Properties (E_γ= 136.5 keV)

E_γ= 136.46 ± 0. 05 keV
$t_{1/2}(\gamma M)$ =8.7 ± 0.4 ns)
$\alpha_T(\gamma M)$ =0.1
$\rho(\gamma M)$ =12 %
MM = +0.88 ± 0.05 nm

Figure 2.11 : Decay Scheme of ^{57}Co MÖssbauer Source

* Due to its high abundance (≈2.17 %) of Fe^{57} one can avoid the use of enriched absorber.
* Being a transition metal element the magnetic properties can be measured with this technique.

2.14 MÖSSBAUER PARAMETERS:

In a solids there are various hyperfine interaction that shift or split the nuclear energy levels and the principal use of the Mössbauer spectroscopy is to study these interactions. Using Mössbauer spectroscopy, the following interaction between the nucleus and the surrounding electrons and ions are of important[5].

(i) electrostatic interaction of the nuclear charge with the surrounding electrons and ions, which results the 'isomershift' and 'quadrupole splitting' of the spectral lines and

(ii) Magnetic interaction of magnetic moments of nuclear energy levesl I=(3/2)$^-$ and I=(1/2)$^-$ with the magnetic field, H_{int}, at the nucleus. This results into the 'Zeeman splitting' of spectral lines.

The parameters isomershift (δ), quadrupole splitting (ΔE) and Nuclear Zeeman splitting that result because of hyperfine interaction, are known as 'Mössbauer parameters'.

In Mössbauer experiment, the source and absorber nuclei are moved relative to each other in a controlled fashion and registers the transmitted γ-quanta as a function of relative Doppler velocity. The plot of the relative transmission versus Doppler velocity shows maximum resonance at relative velocities where emission and absorption lines overlap. From the observed Mössbauer spectrum following various parameters can be obtained.

A brief description of some of these parameters are given below.

2.15 (a) ISOMERSHIFT:

In a given solid, electrons have uniformly spherical distribution. A change in s-electron density at the nucleus due to a coulombic interaction between electron and the nuclear charges gives rise to shift of nuclear levels between source and absorber[6]. This change in a nuclear transition energy is known as "isomershift'. It is also known as "chemical shift".

Isomershift of a given nucleus of a charge Ze is given as

$$\delta = \frac{2\pi}{5} Ze^2 \left[|\psi_a(0)|^2 - |\psi_s(0)|^2 \right] \left(R_{ex}^2 - R_{gd}^2 \right) \quad (7)$$

Above Equation 7 can be also written as

$$\delta = A_N e \left(|\psi_a(0)|^2 - |\psi_s(0)|^2 \right) \quad (8)$$

where, $A_N = \frac{2\pi}{5} Ze\left(R_{ex}^2 - R_{gd}^2\right)$ is a function of nuclear parameters, R is a radius of a excited (ex) and ground state (gd). $e|\psi(o)|^2$ is a s-electron density for absorber 'a' and source 's'.

Isomershift 'δ' is related to the local environment surrounding the source and absorber nuclei, which is also related to binding and covalency of atoms.

In inorganic glasses, the short range order is retained and therefore not much variation in the values of δ, which is predominantly determined by the nature of neighbour ions, from site to site is expected. Several workers, e.g. Kurkjain and Sigety[7], Kurkjain[8], Taneja and Kimbal[9] and Wong and Angel[10] have used these average values of δ to find out the coordination and valence states of iron in glasses by comparing with corresponding values for their crystalline counterparts.

In an iron Mössbauer spectroscopy, Fe^{+2} and Fe^{+3} both can exist in octahedral and tetrahedral sites. Fe^{+2} has larger value of δ as compared to Fe^{+3} because its s-electron density is larger than Fe^{+3}. Following Table 2.11 gives

the idea about different valence state and its corresponding isomershift values in the oxide glasses[8].

Table 2.11: Range of values of isomershift δ for various iron states and coordination.

Charge State & Coordination of iron	Range of δ(mm/sec) w.r.t. Fe metal.
Fe^{+3} (O)	0.39 – 0.52
Fe^{+3} (T)	0.20 – 0.35
Fe^{+2} (O)	0.90 – 1.30
Fe^{+2} (T)	0.80 – 0.95

2.14 (b) QUADRUPOLE SPLITTING:

The electric quadrupole splitting arises due to the interaction between nuclear quadrupole and the field gradient q due to charge present in the surrounding of a crystal. The nuclear state with I>1/2 have only nuclear quadrupole moment. The measure of nuclear quadrupole moment Q gives a deviation from spherical symmetry of a nuclear charge. In an iron Mössbauer spectroscopy, ground state of Fe^{57} with I=1/2 does not possess any quadrupole splitting because it has spherical charge distribution with zero quadrupole moment (Figure 2.12). The states I=3/2 have non-spherical charge distribution and possess finite quadrupole moment Q.

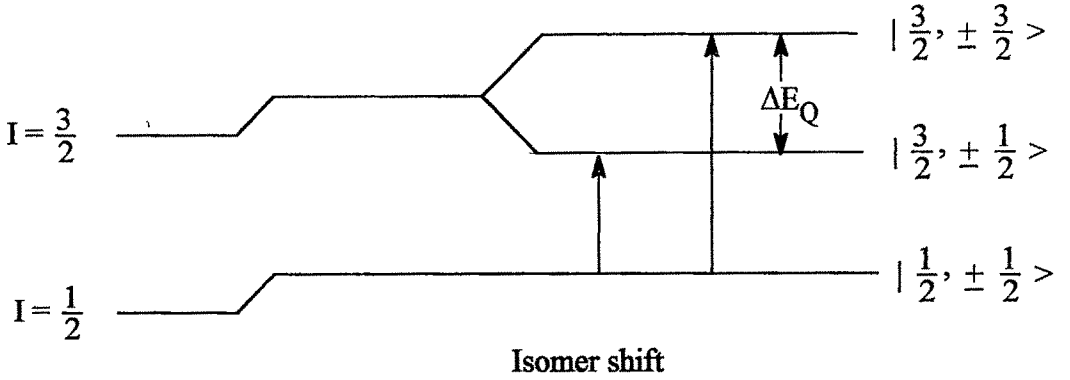

(a)

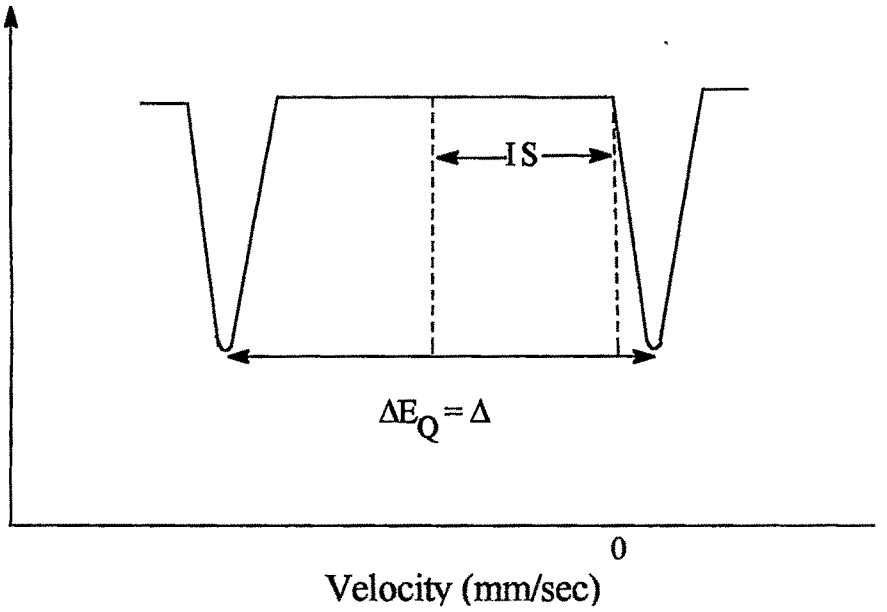

(b)

Fig. 2.12: (a) Electric quadrupole splitting of ^{57}Fe
(b) The resultant Mossbauer spectrum representing the measurement of quadrupole splitting

The electric quadrupole interaction splits the first nuclear excited state of Fe^{57} (I=3/2) into sublevels, as indicated in the energy level diagram.(Figure 2.12) with the eigen values

$$E_Q = \pm(¼)eQV_{ZZ}\{1+(n^2/3)\}^{1/2} \quad (9)$$

Where, n is given by $n = (V_{XX}-V_{YY})/V_{ZZ}$

With, $|V_{ZZ}| \geq |V_{YY}| \geq |V_{XX}|$; $V_{ZZ}+|V_{YY}+V_{XX} = 0$ (10)

The quadrupole splitting ΔE_Q for state I=3/2 is given by

$$\Delta E_Q = E(\pm 3/2) - E(\pm 1/2) = (1/2)e^2qQ \quad (11)$$

Equation 11 gives ΔE_Q experimentally. As Fe^{+3} ion is a spherically symmetric, it does not give any electric field gradient at the nucleus. The finite value of ΔE_Q ($\neq 0$) for Fe^{+3} indicates the deviation from cubic symmetry. The electric field gradient (e.f.g) due to surrounding ions (lattice) is denoted by q_{latt} is

$$q(Fe^{+3}) = q_{latt}(1-\gamma_\alpha) = (1-\gamma_\alpha)/4\pi\varepsilon_o \quad (12)$$

where γ_α is the antishielding factor for the polarization of $3d^5$ core. For non-spherical charge distribution of valence electron in Fe^{+2} have an additional contribution[11], hence

$$q(Fe^{+2}) = (1-R)q_{lval} + (1-\gamma_\alpha)_{latt} \quad (13)$$

Where q_{val} is an electric field gradient due to asymmetric charge distribution of valence electron in valence state. R is the Strenheimer shielding factor.

Generally Fe^{+2} has large quadrupole splitting than that of Fe^{+3} as is obvious from Equation 13. According to Levy et. al.,[12] Fe^{+3} at distorted tetrahedral sites exhibits larger ΔE_Q than Fe^{+3} at distorted octahedral sites (Table 2.12). The glasses have been found[8] to possess large ΔE_Q than the corresponding crystals because the distortion in the symmetry of coordination polyhedron in glasses is more. Also, inspite of variation in ΔE_Q at each of the sites, it has been possible to define a unique average value of ΔE_Q in the glass

for each distinguished valence and coordination states. The intensities of both the lines in the quadrupole doublet in glasses are considered to be equal due to the anticipated absence of texture effects[13] and Goldanski-Karaygin effects[14].

Table 2.12: Range of values of quadrupole splitting (ΔE_Q) for different sites of iron.

Charge State & Coordination of iron	Range of quadrupole splitting (ΔE_Q) (mm/sec)
Fe^{+3} (T)	1.1 – 1.4
Fe^{+3} (O)	0.6 – 0.9

2.13 (C) MAGNETIC SPLITTING:

The change in the energy of the state arises due to the presence of external fields on the site of a nucleus having non-zero magnetic moment and the energy change is given by

$$E_M = -\vec{\mu}_H . \vec{H} = g \mu_N H m_Z \qquad (14)$$

where μ_N is the nuclear magneton, g is the nuclear g-factor and m_z is the magnetic quantum number representing the Z-component of the nuclear spin. The magnetic field splits the nuclear level into (2I+1) equispaced sublevels. The transition can take place between different nuclear sublevels if $\Delta m_I = 0, \pm 1$. The allowed transitions for a $3/2 \rightarrow 1/2$ levels are illustrated in Figure 2.13.

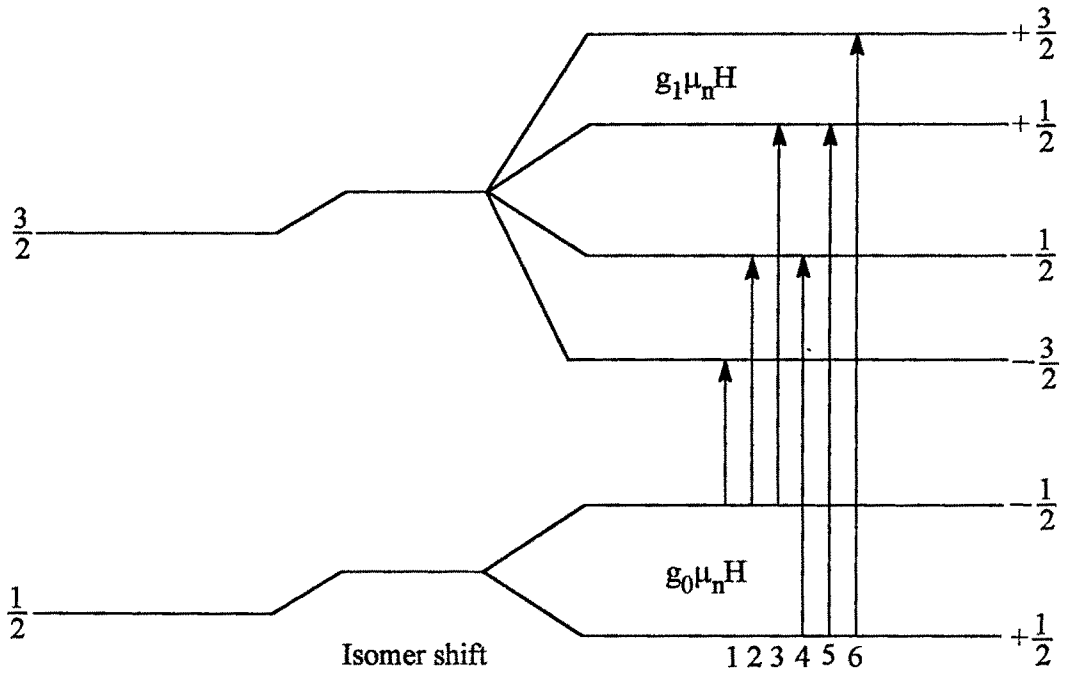

Fig. 2.13: Magnetic Hyperfine Splitting of ^{57}Fe

The resultant Mössbauer spectrum contains a number of resonance lines, but is nevertheless symmetrical about the centroid. The six lines are allowed $\Delta m_z = 0, \pm 1$ transitions and the resultant spectrum is indicated in the Figure 2.14. The lines are not of equal intensity, but the 3:2:1: 1:2:3 ratios. Incase of glasses having zero quadrupole moments these lines are symmetrically located in a spectrum but in the other case with quadrupole interaction the lines are placed symmetrically. The presence of hyperfine splitting in inorganic glasses gives an indication of devitrification of magnetic phase i.e. crystallites of iron[15-16].

2.14 (D) LINE SHAPE AND WIDTH:

In a Mössbauer spectroscopy the resonance absorption shows a characteristics energy dependence of the from

$$I(E) = (\Gamma/2\pi)\,[(E-E_t)^2 + (\tfrac{1}{2}\Gamma)^2]^{-1} \qquad (15)$$

Where Γ represents the full width at half maximum and E_t represents the nuclear transition energy. This type of distribution shows a Lorentzian shape. The nuclear line width of the 14.4 KeV gamma ray of Fe^{57} is 0.19 mm/s. The broadening of lines due to thick absorber, instrumental effect, solid angle effect and the diameter of detector can be reduced to some extent by taking special precautions and using stable equipment[17-19]. The optimum thickness of absorber should be such that it contains 5 mg/cm^2 of natural iron in order to get minimum broadening with high percentage of resonant absorption. The glasses have normally a larger broadening of spectral line as compared to that of a crystalline material due to the variation of iron environment at each of the sites in the glasses.

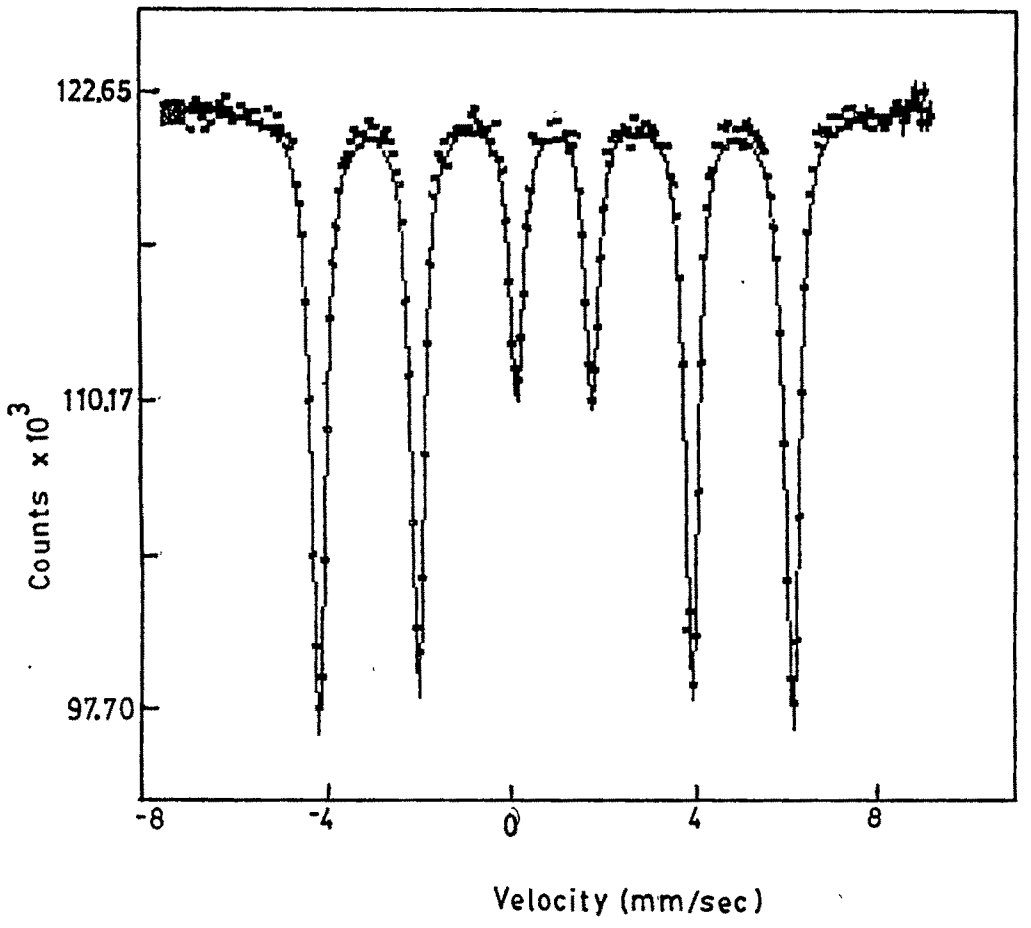

Figure 2.14 : Fe-57 Mössbauer spectrum of Natural Iron foil.

REFERENCES :

1. R. L. Mössbauer , Z. Physik, **151**(1958)124.
2. N. N. Greenwood and T. C. Gibb, Mössbauer Spectroscopy, Chapman and Hall Ltd., London, 1971.
3. V. G. Bhide, "Mössbauer efect and its Applications" Tata-McGraw-Hill, New Delhi, 1973.
4. G. K. Shenoy and F. E. Wanger, Eds. "Mössbauer Isomershift", North-Holland Publishing Co., Amsterdam, 1978.
5. V. I. Goldanskii & E. F. Makarov in "Chemical Applications in Mössbauer spectroscopy", Eds. V. I. Goldanskii & R. H. Herber, Academic, New York, 1968.
6. L. R. Walker, G. K. Wertheim & V. Jaccarino, Phy. Rev. Letters, 4(1960)441.
7. C. R. Kurkjain & E. A. Sigety, Phys. & Chem. Of Glasses, 9(1968)73.
8. C. R. Kurkjain, J. Non. Cryst. Solids 3(1970)157.
9. S. P. Taneja, C. W. Kimball & J. C. Shaffer, in "Mössbauer Effect Methodology" Vol. 8, Ed. I. J. Graverman & C. W. Seidel, Plenum, New York, 1973.
10. J. Wong & C. A. Angell in "App. Spect. Rev." Vol. 4, Ed. E. J. Brame, Marcell Dekker, New York, 1971, p. 97.
11. R. Ingalls, Phys. Rev. **133**(1964)787.
12. R. A. Levy, C. H. P. Lupis & P. A. Flinn, Phys. & Chem. Of Glass, **17**(1976)94.
13. U. Gonser, Ed., "Mössbauer Spectroscopy Mössbauer (Topics in Applied Physics, Vol. 5), Spring Vorlag, New York, 1975.
14. V. I. Goldanskii & R. H. Herber, Eds. "Chemical Applications of Mössbauer spectroscopy ", Academic, New York, 1968.

15. R. R. Bukrey, P. F. Kenealy, G. B. Beard & H. O. Hopper, Phys. Rev. **B9** (1974)1052.
16. R. R. Bukrey, P. F. Kenealy, G. B. Beard & H. O. Hopper, J. Appl. Physc. **40**(1969)4289.
17. J. Herbrele, Nucl. Inst. Methods, **58**(1968)90.
18. S. Margulies & J. R. Ehraman, Nucl. Inst. Methods, **12**(1961)131.
19. S. Margulies, Z. Physik, **176**(1963)63.

2.2 ELECTRICAL CONDUCTIVITY:

2.21 INTRODUCTION:

Certain substances like germanium, silicon, carbon etc. are neither good conductor like copper nor insulator like glass. In another words, the resistivity of these materials lies in between conductors and insulators. Such substances are classified as " semiconductors".

Present chapter leads to understand a conduction mechanism in non-crystalline materials like glasses. Most of all the glasses in common practice are insulating in nature. But, there are some glasses containing transition metal oxides (TMO) show the semiconducting behaviour for higher temperature due to the existence of more than one valence states in transition metal oxide like V_2O_5, P_2O_5, Fe_2O_3 (V^{+4} & V^{+5} in V_2O_5) [1] and transfer of electron from one valence state to other. Many workers studied on the glasses containing transition metal oxides[2-6].

TRANSITION METAL OXIDE GLASSES:

Transition metal oxide glasses are those, which have the major, constituent as transition metal oxide such as V_2O_5, P_2O_5, Fe_2O_3. These glasses are of the charge-charge transfer or mixed valence type of semiconducting conductor. Transport in these glasses requires at least two of its valence states and conduction occurs by the transfer of an electron from a reduced to a more oxide ion[1] e.g. $V^{+4} \rightarrow V^{+5}$. Consequently the conduction is through the d-levels of the transition metal and as the d-overlap is small, the bandwidth is also small, the effective mass m^* is large and the electron wavelength $\lambda = h/(2\pi m^* kT)^{1/3}$ is of the order of lattice spacing. The electron is, therefore, essentially localized and almost certainly self-trapped through the formation of

small polaron conduction occurred by hopping but localization due to disorder makes a contribution to conduction too. The activation energy W becomes $W_H + \frac{1}{2}W_D$ and W_D the disorder energy. Also, the carrier concentration n of transition metal ions is proportional to c(1-c), where c is the ratio of reduced to total content of the transition metal ion (V^{+4}/V_{total}). I. G. Austin and N. F. Mott (1969)[7] described a conduction mechanism in non-crystalline solids and subsequently many workers had worked to understand the conduction mechanism for non-crystalline materials. Anderson et. al. (1958) [8] had given a clear picture about localization of electron and Miller & Abraham [9] in 1960 gave a mechanism of conductivity in a Si and Ge. An electron in a non-crystalline solids moves by thermally activated hopping from one localized state to another one and an activation energy associated with this hopping due to localization of its state is quantized energy for a certain range. An exchange of energy with phonon causes the localization.

The present work of electrical conduction in semiconducting glasses is based on the theories of Mott and Austin [7]. Many workers [7-12] had worked on such type of materials and suggested the carrier mechanism in such materials be due to small polaron.

2.22 SMALL POLARONS:

Holstein and Friedman [10] developed a small polaron theory and a mechanism of conduction was studied by many workers [8-14]. The polaron is a concept which consists of the electron which occupies each site, in its motion through the crystal for a time sufficiently long to relax into a configuration appropriate to the alter charge on the host ion than the typical period of vibration. This electron and its accompanying distortion is termed as a single entity, called the polaron [10-11]. If the size of this polaron is greater than the

radius of the ion on which the electron is localized, but less than the distance separating this and neighbouring site, such a polaron is called "Small Polaron".

2.23 SMALL POLARON CONDUCTION MODEL:

A conduction mechanism in a non-crystalline materials by small polaron hopping was discussed by Mott & Austin in 1968 [7,15] . To explain a conduction mechanism in non-crystalline materials, following model based on a Mott's theory is used.

If a carrier remains for a sufficiently long time on a particular atomic or ionic site (i.e., V^{+5}) than the period of vibration, then the ions in the neighbourhood of this excess charge will get enough time to get a new equilibrium position consistent with the presence of this additional charge. This will generate potential well for additional carriers. A carrier may bound to a state due to a deep potential well. Thus a bound carrier and its induced lattice deformation in a solid is termed as a *"Polaron"*.

A polaron is said to be small if a potential well is localized at a single atomic or ionic site. Figure 2.21 gives a clear picture of this model.

As shown in Figure 2.21 (a) initially an electron is trapped in a potential well and the smallest activation energy corresponds to this state is given in Figure 2.21 (b), when it is thermally activated. The energy required for this is given by

$$W_H = \tfrac{1}{2} W_P = e^2/4\varepsilon_p \nu_p \qquad (1)$$

Where $\varepsilon_p = [(1/\varepsilon_\alpha) - (1/\varepsilon_s)]^{-1}$, ε_S and ε_α are the static and high frequency dielectric constants of the material, ν_p is the polaron radius and W_H is the activation energy.

Electron hopping process between a and b ions when the states are localized, ν_p is the polaron radius i.e., a distance from the electron beyond which the medium is polarized.

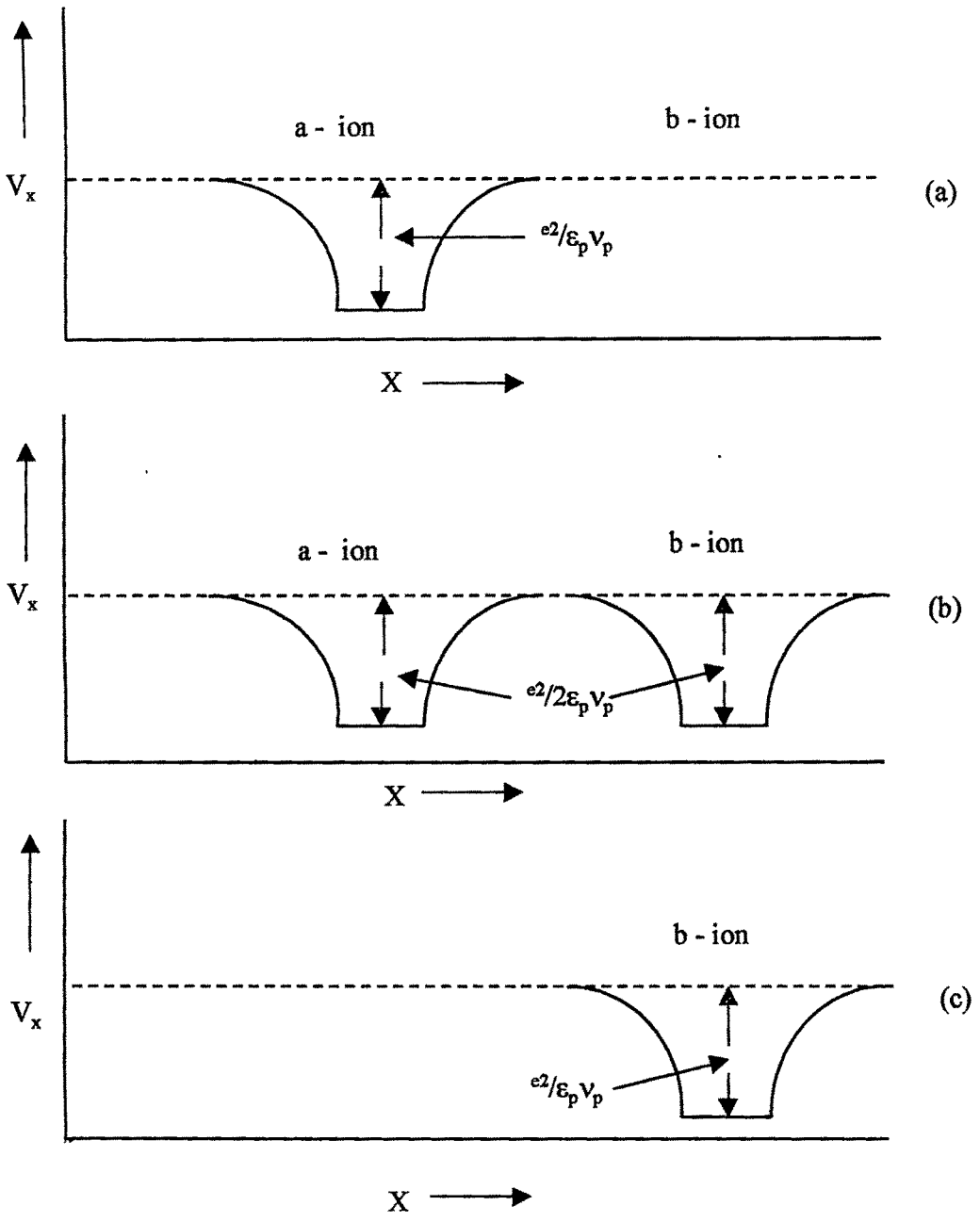

Figure 2.21: Picture of Small Polaron Conduction Model.

Thus trapped electron produces a potential well of energy given by

$$v_p(r) = e^2/\varepsilon_\alpha r \qquad \text{for } r > v_p$$

After the ions are displaced, the potential energy becomes $e^2/\varepsilon .r$.

Thus an electron "digs" a potential well for itself for which

$$v_p(r) = -e^2/\varepsilon_p r \qquad \text{for } r > v_p \qquad (2)$$

$$= e^2/\varepsilon_p v_p \qquad \text{for } r < v_p$$

The value of v_p can be determined by minimizing the kinetic energy of the electron i.e., by localized state.

2.23 (A) LOCALIZED STATES:

At a given density of electrons N(e), the mobility of electron is zero at a finite E, i.e., $\sigma_E(0)$ vanishes for these energies then the electron is said to be localized with energy E. If states are localized, mobility μ vanishes at T=0. At finite temperature, the mobility is essentially due to interaction with phonons. In principle, localization ($\sigma_E(0) = 0$) can occur for a given energy E for the following reasons.

(a) A random potential at each atom [3]

(b) Fluctuations in the density or mean interatomic distance.

(c) Absence of long-range order.

(B) SMALL POLARON AND LARGE POLARON HOPPING:

When a state is localized we consider two approximation for hopping after determining v_p.

(i) The effective mass m^* of the electron is too high and the kinetic energy becomes very small. Then v_p must be less than the interatomic distance ($v_p < R$) and the polaron is said to be ***"small polaron"***.

In this case total potential energy of the electron becomes

$$W_P = \frac{1}{2}\left(\frac{e^2}{\varepsilon_P v_P}\right) \qquad (3)$$

(ii) For $v_p > R$, the polaron hopping becomes a "large polaron" due to smaller m^*. In this case total energy is given by

$$W_P = \left(\frac{e^2}{\varepsilon_P v_P}\right) + \left(\frac{h^2\pi^2}{2m^* v_P^2}\right) \qquad (4)$$

Equation 4 will be minimum when

$$v_P = \frac{2\pi^2 h^2 \varepsilon_P}{m^* e^2} \qquad (5)$$

Equation 1 is corrected for larger value of R i.e., distance between the centre. Therefore, for a larger value of R, two polarization clouds overlap and W_H becomes dependent on jumping distance R. Mott in 1968[16] modified Equation 1,

$$W_H = \left(\frac{1}{4}\right)\left(\frac{e^2}{\varepsilon_P}\right)\left[\frac{1}{v_P} - \frac{1}{R}\right] \qquad (6)$$

Polaron radius for a crystalline material is given by

$$v_p = \tfrac{1}{2}(\pi/6N)^{1/3} \qquad (7)$$

where N is the number of sites (i.e., V_{total} ions in V_2O_5) per unit volume. For a larger number of sites the polaron becomes smaller in size.

(C) ADIABATIC AND NON-ADIABATIC HOPPING PROCESS:

For a non-crystalline solids having a disordered system with disorder energy W_D, activation energy and the total activation energy for hopping process are related by

$$W \approx W_H + \tfrac{1}{2}(W_D) \qquad \therefore W_D < W_H \qquad (8)$$

For a disordered lattice, the coincidence of electronic energy level of the bound electron sites with the local electronic energy level on neighbourhood

gives rise to transfer of a small polaron. This transfer probability is given by,

P = probability of coincidence x (Probability of transfer when coincidence occurs)

$$= (\omega_o/2\pi) \exp(-\omega/kT) \times p \qquad (9)$$

where p is probability of transfer when coincidence occurs, which is related to two types of cases;

(a) Adiabatic Hopping Process:

In this case, an electron always follows the lattice motion. If the value of p is;

(i) equal to unity (p=1) for a time duration of coincidence event is long compared with the time it takes an electron to transfer between two sites and electron always follows lattice motion.

(ii) less than unity(P<<1) when the time required for an electron to hop is larger compared to duration of coincident event and electron will not always follow lattice motion.

Value of p is given by [12]

$$p = (2\pi/h\omega_o)[\pi/2W_H kT]^{1/2} J^2, \qquad (10)$$

where J is the electron transfer integral and is a measure of wave function overlap of the neighbouring sites. If $J>h\omega_o$ and the tunneling probability $\exp(-2\alpha R)$ is small where α is a spatial decay constant of electron wave function, hence conduction is due to adiabatic hopping.

(b) Non-Adiabatic Hopping Process:

A non-adiabatic hopping process would occur if $J<h\omega_o$ (i.e., predominant phonon energy). Hence p contains the factor $\exp(-2\alpha R)$.

Thus, it is clear from these two cases and by using[10] Equation 9

$$J \gtrless \left[\frac{2kTW_H}{\pi}\right]^{1/4}\left[\frac{h\omega_o}{\pi}\right] \quad \begin{matrix} \text{adiabatic } (>) \\ \text{Non-adiabatic } (<) \end{matrix} \qquad (11)$$

The polaron band width J can be estimated from the difference of mean value of hopping energy and the experimental activation energy W. By finding value of J, the nature of hopping in several glasses were also reported [5,7,13-15,17].

2.24 ELECTRICAL CONDUCTION IN NON-CRYSTALLINE MATERIALS:

N. F. Mott (1969)[7] gave theory for electrical conduction in non-crystalline solids containing transition metal oxides, which is as following.

$$\sigma = \left[\frac{\nu_o e^2 c(1-c)}{kTR}\right] \exp(-2\alpha R)\, \exp(-W/kT) \qquad (12)$$

where c is the ratio of the concentration of low valence ions to the total concentration of transition metal oxides. ν_o is the optical phonon frequency in the range of $10^{11} - 10^{13}$ Hz. R is the average spacing between two sites and $\exp(-2\alpha R)$ is the integral overlap function which is approximately equal to $J^2 \approx \exp(-2\alpha R)$. It is also called as polaron bandwidth or tunneling probability factor for electron. α is a spatial decay constant for electron wavefunction.

Comparing Equation 12 with Arrhenious Equation [7]

$$\sigma = \sigma_o \exp(-W/kT) \qquad (13)$$

We get,

$$\sigma_o = \left[\frac{\nu_o e^2 c(1-c)}{kTR}\right] \exp(-2\alpha R) \qquad (14)$$

Where σ_o is a pre-exponential term for conductivity and can be estimated from conductivity data. Value of α can also be calculated from the above Equation. 14.

The temperature dependence of conductivity for the transition metal oxide was well explained on the basis of theory developed by Schnakenberg [18]. According to which the activation energy, W, continuously decreases with the temperature and this type of behaviour was found for a small polaron hopping in amorphous transition metal oxides.

As from Equation 11, if a plot between logσ and W gives a slope of a line equals to $-1/2.303kT$, the tunneling term $\exp(-2\alpha R)$ could be negligible and the adiabatic approximation can be considered. If it differs much from the said value, non-adiabatic approximation can be considered [19]. Thus the equation for conductivity in non-crystalline solids carries a great importance and gives a clear picture of conduction in such types of materials.

REFERENCE:

1. N. F. Mott & E. A. Davis, "Electronic process in non-crystalline materials" Oxford Univ.,press (1971)
2. G. S. Linsley, A. E. Owen & F. M. Hayete, J. of Non-Cryst. Solids, **4**(1970)208.
3. M. Sayer & A. Mansingh, Phys. Rev. **B6**(1972)4629.
4. M. Sayer, A. Mansingh, J. M. Reyes & G. Rosenblatt, J. Appl. Phys. **42**(1971)2857.
5. V. K. Dhawan & A. Mansingh, J. of Non-Cryst. Solids, **51**(1982)87.
6. A. Mansingh, V. K.. Dhewan, R. P. Tandon, & J. K. Vaid, J. of Non-Cryst. Solids, **27**(1978)308.
7. I. G. Austin & N. F. Mott, Adv. Phys., Vol. **13**, No. 17 (1969)41.
8. P. W. Anderson, Phy. Rev. **109**(1958) 1492.
9. A. Miller & E. Abraham, Phy. Rev. **120**(1969)745.
10. T. Holstein, Ann. Phys. **8** (1959)325.
11. A. P. Schmid, J. of Appl. Phys.,Vol. **39**, 7(1968)3140.
12. Murawaski, C. H. Chung and J. D. Mackenzie, J. of Non-Cryst. Solids, **32**(1979)91.
13. Hiroshi Hirashima et. al. J. Amm. Ceram. Soc. **68**, 9(1985)486.
14. A. Ghosh & B. K. Chaudhari, J. of Non-Cryst. Solid. **83**(1986)151.
15. I. G. Austin, J. of Non-Cryst. Solids **2**(1970)474.
16. N. F. Mott, J. of Non-Cryst. Solids,**1**(1968)1.
17. M. Sayer & A. Mansingh, J. of Non-Cryst. Solids, **58**(1983)91.
18. Schnakenberg, J. of Phys. Z, **185**(1965)123.
19. H. R. Panchal, D. K. Kanchan & D. R.S. Somayajulu, J. of Mater. Sci. Forum, Vol. 223-224(1996)304.

2.3 ELECTRICAL SWITCHING

2.31 INTRODUCTION:-

Semiconducting glasses often show marked deviation from normal semiconductor behaviour, e.g., non-ohmic conduction under the influence of temperature and or in a strong electric field to a free charge carrier system may influence both the mobility of the carriers and the number of available carriers. The mobility of the carrier may be influenced by the change in the effective energy distribution of the carriers, which would be described in terms of a rise of carrier temperature, T_c, above the lattice temperature. In a Semiconducting glass, the ohmic behaviour is observed for low voltages whereas for intermediate voltage the current through the samples increases abruptly and non-ohmic behaviour is observed. The rapid increase in the current without any significant increase in the applied voltage can be used as a switching. Various mechanisms, proposed for the switching of Semiconducting glasses[1-4] can be divided into two groups; one is electrothermal and the other is electronic. In order to elucidate the switching mechanism, it is important to examine which initiates switching, the increase of conductivity by electrothermal heating or the increase of current by the electronic effect at a high field (or voltage).

The characteristics of switching are known to be influenced by several factors like pretreatment, addition of transition metal oxides, construction of electrodes, distance between electrodes, applied voltage, ambient temperature and so on. The electrothermal switching was reported to work when the distance between electrodes was relatively large[5]. When the applied voltage or field is sufficiently raised, the observed switching is electronic origin. Basically there are two types of switching; one is threshold switching and other is memory switching. Many authors [6-8] have attempted to explain the

switching phenomenon on the basis of thermal process, whereas other[9-10] have attempted electronic approach to this mechanism. Transition metal oxide glasses, because of their semiconducting properties[11], show electrical threshold as well as memory switching effects [12-15]. Different mechanism have been proposed inorder to explain switching process in these type of glasses [6,16].

2.32 SWITCHING EFFECT:

It has been known for many years that when the interelectrode distance in samples of amorphous or glassy semiconductor is reduced to sufficiently small values (typically a few μm), the current voltage characteristics are no longer governed by ohms law after a certain threshold voltage has been reached. At this point a partial breakdown takes place and the conduction of the sample appears to increase abruptly. This phenomenon is described as a ***"switching effect"***. A similar behaviour was observed in glasses of various compositions at varying temperature. It is observed that the conduction is ohmic at low fields, but at higher fields the current increases rapidly with the voltage establishing non-ohmic type conduction. When the applied voltage exceeds a certain threshold voltage V_{th}, breakdown occurs and the device switches for a high resistance [off-state] to a low resistance [on-state]. A rapid increase in current and a huge drop in voltage across the sample occurs. As the applied voltage is increased further, the current continues to increase.

There are two types of switching [8-9]

(a) Electrical switching and

(b) Memory switching

In both types, the switching process occurs when an increasing applied voltage exceeds the threshold voltage V_{th}, or after a delay time, t_D, when a voltage pulse, V_p, larger than V_{th} is applied. The switching process takes place

very rapidly within a switching time is $t_s < 10^{-10}$ sec. However, there is a delay time t_D, typically about 10^{-6} sec at the threshold voltage and the delay time decreases exponentially with over voltage[17].

In case of thermal switching, if the holding voltage is removed the device switches back to the high resistance state [off-state] in about 5 x 10^{-7}sec[16]. The switching process is reversible and independent of polarity. The threshold voltage decrease with increasing the temperature and it has been reported[18] that the threshold voltage appears to increase exponentially with glass transition temperature for larger number of disordered materials. The exponential decrease of threshold voltage with temperature is reported to be an indication of thermal phenomenon caused by Joule's heating which is responsible for switching in these type of glasses[19].

At low fields the conductivity is low and obeys ohm's law until the applied voltage reaches the threshold voltage. Above this voltage, after a delay time, there is rapid switching from high resistance [off-state] to low resistance [on-state][20]. After switching, if the current is quickly reduced to below a critical value the device will switch back to the high-resistance state, exactly like a electrical switch. However, if the device is held in the conductive state for about 10^{-3} sec, it will remain highly conductive, even after the external field is removed. This time is called the lock-on-time (t_l). Memory switched material can usually be returned to the original high resistance [off-state] by applying a short instant current pulse of either polarity.

It is known that during a memory switching process, a crystalline channel is formed between the electrodes at the switching voltage [6,21], giving rise to a low-resistance state. The high current resetting pulse succeed in melting the crystalline material and cools it rapidly into a glassy state. A decrease in the threshold voltage with the increase in temperature supports the idea that a thermally generated crystalline material is responsible for switching. As the temperature is increased, molecular rearrangement and relaxation

becomes easier in the glasses, which causes further formation of crystalline filament. According to Cohen et al.[22], the voltage in the high resistance state is increased, the current becomes increasingly non-ohmic due to self-heating. The conductivity increases and a rise in the internal temperature yields a collapse of the current region into a filament at a critical temperature at which devitrification takes place.

Jackson and Shaw[23] have reported a theoretical model for ideal thermal switching in which a sudden decrease in resistance of the device occurs at the glass transition temperature T_g. According to which, the breakdown conditions reached when the temperature along the central axis of the sample becomes equal to the ambient temperature.

Both the types of switching have important applications in the electronic industries and other areas of engineering.

REFERENCES:

1. N. F. Mott., Contemp. Phys. **10**(1969)125.
2. N. F. Mott., Phil. Mag. **24**(1971)911.
3. W-Van Roosbroeck, J. of Non-Cryst. Solids, **12**(1973)232.
4. M. Fritzsche, Electronic and structural properties of Amorphous semiconductor eds P.G Le Comber and J. Mort. (Academic Press, London, 1973), p.557.
5. A.C. Warren IEEE Trans. Electron. Dev. ED-**20**(1973)123.
6. J. k. Higgin and B. K. Temple and J. E. Lewis, J. of Non-cryst. Solids, **23**(1977)187.
7. H. J. Stocker, C. A. Barlow Jr. and D. F. Weirauch, J. of Non-Cryst. Sol., 4(1970)523.
8. S. R. Ovshinsky, Phy. Rev. Lett. 21 (1968)1450.
9. D. R. Haberland, Sol. Stat. Elec. 13(1970)207.
10. R. P. Shanks, J. of Non-Cryst. Solids, 2(1970)504.
11. I. G. Austin and N. F. Mott. Adv. Phys. 18(1969)41.
12. C. F. Darke, L. F. Scanlan and Engel. A.; Phys. Stat. Solidi, **32** (1969)193.
13. A. Mansingh and R. Singh, J. Phy. C. **13** (1980)5725.
14. A. Mansingh, R. Singh and J. B. Krupanidhi, Sol. St. Electron, **23** (1980)649.
15. A. Mansingh, J. K. Vaid and R. P. Tandon, Phy. St. Solidi (a) **38**(1976)K1.
16. A. A. Hosseini and C. A. Hogarth, J. of Mat. Sci., **20**(1985) 261-268.
17. A. Csillay and H. Jager, J. of Non-Cryst. Sollids, 2(1970)123.
18. S. Liziam, M. Sugi, M. Kikuchi and K. Tanaka, Sol. Stat. Com. 8(1970)153.
19. K. W. Boer and S. R. Ovshinsky, J. of Appl. Phy. 41(1970)2675.

20. Aswin Ghosh, J. Appl. Phy. 64(5)1, Q.2652.

21. E. Gatt and Y. Dimitriev, Phil. Mag. B. 40,233(1979).

22. M. S. Cohen, R. G. Neale and A. Paskin, J. of Non-Crys. 8-10,885(1972).

23. J. L. Jackson and M. P. Shaw, Appl. Phys. Lett. 25,666(1974).

2.4 INFRARED SPECTROSCOPY:

2.41 INTRODUCTION:

Infrared spectroscopy is a fundamental technique for chemical identification of a functional group, which provides an useful information regarding structure of molecules. A chemical substances shows a selective absorption of IR radiation, which is due to changes of vibrational and rotational stages and gives rise to closely packed absorption band called an IR absorption spectrum. Different bands, observed in IR spectrum correspond to various functional groups and bonds, found in chemical molecules. The IR spectrum of a molecule may be considered as its fingerprint and can be used for the identification of the compound.

The ordinary infrared spreads over from 2.5μ to 15 μ [1μ= 10^{-4} cm]. The region lying between 0.8μ to 2.5μ is known as ***"near infrared region"*** and that lies between 15μ and 200μ is called the ***"far infrared"*** region[1].

The absorption of IR can be expressed either in terms of wavelength λ or wave number ν. In most of the cases the, IR spectra are plotted as percentage of transmittance against wavenumber. IR absorption takes place in a region of longer wavelength, whereas ultraviolet and visible absorption occurs at shorter wavelength region. The longer wavelengths requirement arises from vibrational stretching and bending of atomic bonds within the molecule as well as from molecular rotations. The ultraviolet and visible absorption bands are primarily because of electronic transition. The broad absorption bands generally characterize ultraviolet and visible spectra, whereas sharp bands characterize infrared spectra.

2.42 REQUIREMENTS FOR ABSORPTION OF INFRARED RADIATION:

Those molecules, which fulfil the following conditions, absorb infrared radiation.

(a) Correct wavelength of radiation:

Only those molecules can absorb radiation in which the natural frequency of vibration of molecules is the same as the frequency of incident radiation. The IR radiation, that is absorbed, causes the molecule to vibrate at increased amplitude (Resonance).

(b) Electric Dipole:

Only those molecules can absorb IR radiation in which absorption produces some changes in the electric dipole of the molecules. Such molecules are known as IR active materials. When a molecule having electric dipole is kept in the electric field, it exerts a force on the electric charges in the molecules, which gives rise to decrease or increase of a separation. Change in the electric field of IR radiation causes a change in polarity periodically, it means that the spacing between the charged atom of the molecule also changes periodically and vibration of these charged atom causes the absorption of IR radiation.

2.42 THEORY OF IR ABSORPTION SPECTROSCOPY:

Molecules are consisting of atoms, which are not stationary. They continuously rotating and vibrating in a number of ways.

Two atoms are joined by a covalent bond which may undergo stretching vibrations. Three atoms can undergo a variety of stretching & bending

vibrations.

Energy of vibration depends on

(a) The mass of atom present in a molecule:

Light elements vibrate at higher frequency as compared to heavier elements.

(b) Strength of the bonds:

Triple bonds are stiffer than double and single bonds. Hence, they vibrate at higher frequency than the double and single bond.

(c) The arrangement of various atoms in the molecules:

The position of IR bond is given in terms of wavelength λ or wave number ν (cm^{-1}), which are related by

$$\nu\ (cm^{-1}) = 10^4/\lambda\ (\text{in } \mu) \qquad (1)$$

In case of diatomic harmonic oscillator the position of absorption band is[2]

$$\nu\ (cm^{-1}) = \left(\frac{1}{2\pi c}\right)\left[\frac{k(m_1+m_2)}{m_1+m_2}\right]^{1/2} \qquad (2)$$

Where k is a force constant and is expressed in dyne/cm, m_1 and m_2 are the masses of the adjacent atoms in a molecule. The force constant cab be expressed as

$$k = aN\left(\frac{\chi_1\chi_2}{d^2}\right)^{3/4} + b \qquad (3)$$

Where, N is the bond order, χ_1 and χ_2 are the electronegativity of the atoms, d

is the internuclear distance in Angstroms. a (≈1.67) and b (0.30) the constants.

The Equation 2 can also be written in terms of atomic weights of the two atoms.

$$\nu\,(\mathrm{cm}^{-1}) = 1303\left[\frac{1}{M_1}+\frac{1}{M_2}\right]^{1/2} \qquad (4)$$

Where, $1303 \approx [1/2\pi c\ (N \times 10^3)]^{1/2}$, N is the Avagadro number (6.023×10^{23}).

Molecules in a given compound possess different kinds of vibrations like stretching, bending, etc. and are also rotating.

2.431 STRETCHING VIBRATION:

Stretching vibrations arise due to stretching and contracting of bonds without producing any change in bond angles, which are of two types.

(i) Symmetric Stretching:

If the movement of atoms with respect to a particular atom in a molecule is in the same direction as shown in Figure 2.41, it is called symmetric stretching vibration.

(ii) Asymmetric Stretching:

If one atom approaches the central atom whereas other approaches away from it (Figure 2.42) in a triatomic system, it gives unequal movement of the outer atom with respect to central one. Because of this the change in electrical dipole take place. Therefore, the asymmetric stretching gives it vibrational frequency at higher wave number than for symmetric vibration.

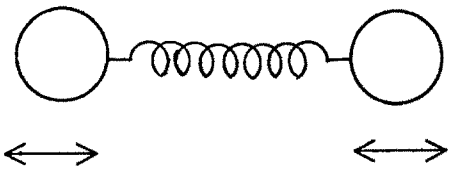

(a)

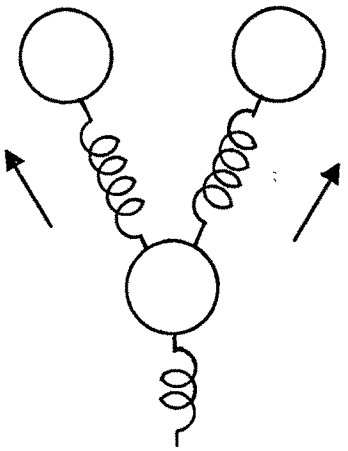

(b)

Figure 2.41: Symmetric Stretching Vibrations:
(a) Diatomic Molecule (b) Triatomic Molecule.

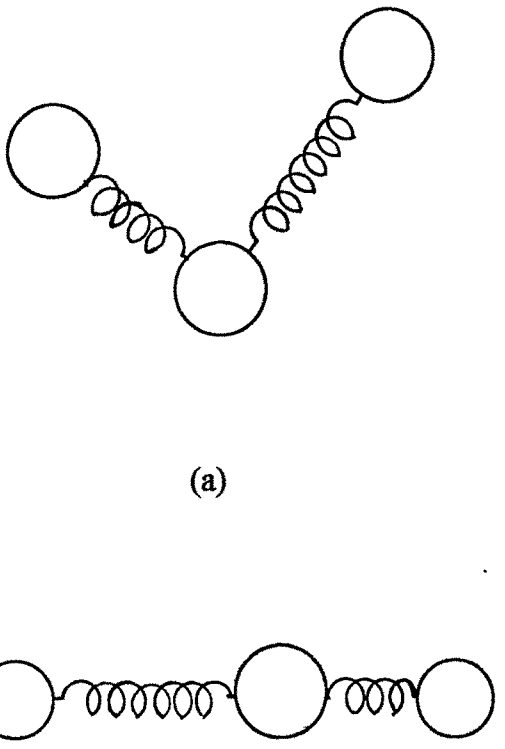

(a)

(b)

Figure 2.42: Asymmetric Stretching Vibrations:
(a) & (b) Triatomic Molecule.

2.432 BENDING VIBRATIONS OR DEFORMATIONS:

Bending vibrations give rise to a deformation of bond angle but there is no change in bond length.

In molecules, most of the bond angles are found to be in two categories.

(i) Linear or 180° bond angle.

(ii) Bond angle in a neighbourhood of 120° to 110°.

In case of triatomic molecules, the two atoms are the same and are bound to the middle atom by two equal bonds with two different frequencies symmetric or asymmetric.

$$\nu_{sym}\,(cm^{-1}) \approx \left(\frac{1}{2\pi c}\right)\left[k\left\{\frac{1}{m_{end}}+\frac{(1+\cos\alpha)}{m_{mid}}\right\}\right]^{1/2} \qquad (5)$$

$$\nu_{asym}\,(cm^{-1}) \approx \left(\frac{1}{2\pi c}\right)\left[k\left\{\frac{1}{m_{end}}+\frac{(1-\cos\alpha)}{m_{mid}}\right\}\right]^{1/2} \qquad (6)$$

Where α is a bond angle, ν is a frequency in cm^{-1}, k is the force constant in dyne/cm, m_{end} and m_{mid} are the masses of one end and middle atom respectively.

The above Equation 5 & 6 can also be written as

$$\nu_{sym}\,(cm^{-1}) \approx \left(\frac{1}{2\pi c}\right)\left[k\left\{\frac{1}{M_{end}}+\frac{(1+\cos\alpha)}{M_{mid}}\right\}\right]^{1/2} \qquad (7)$$

$$\nu_{asym}\,(cm^{-1}) \approx \left(\frac{1}{2\pi c}\right)\left[k\left\{\frac{1}{M_{end}}+\frac{(1-\cos\alpha)}{M_{mid}}\right\}\right]^{1/2} \qquad (8)$$

Where M_{end} and M_{mid} are the atomic weights of end atom and middle atoms.

In the present work, the IR study of potassium boro-vanadate glasses has been done. A number of boro-vanadate, barium vanadate and barium boro-vanadate glasses were studied [3-5]. In these glasses, the vibrational frequency of a bond V-O-V type can be given by [3] Equation 7 and 8.

Where $M_{end} = M_v$ and $M_{mid} = M_o$ are the atomic weights of vanadium and oxygen atoms respectively. α is a bond angle (always greater than 90°) between V-O-V bonds (Figure. 2.43 and 2.44).

In glasses, the bands are generally broader and overlapping than those observed in the crystalline materials. This is because of the lack of long range order in glasses and is similar to the broadening of the spectra observed in other techniques. (e.g., X-ray diffraction, Mössbauer spectra) [6-9].

Bending vibrations are further classified as

(i) Scissoring Bending:

In this type of vibrations of the bonds, the two atoms approach each other in the same plane as shown in Figure 2.43(a).

(ii) Rocking Banding:

In this type of bond vibrations the movement of atom occurs in the same direction and also in the same plane [Shown in Figure 2.43(b)].

(iii) Wagging Bending:

In this type of bonding vibrations the two atoms move up and down below the plane with respect to the central atom as shown in Figure 2.44(a).

(iv) Twisting Bending:

In this type, one of the atom moves up the plane and the other moves down the plane with respect to the central atom [Figure 2.44(b)].

Here + and – sign represents motion above and below the plane of the

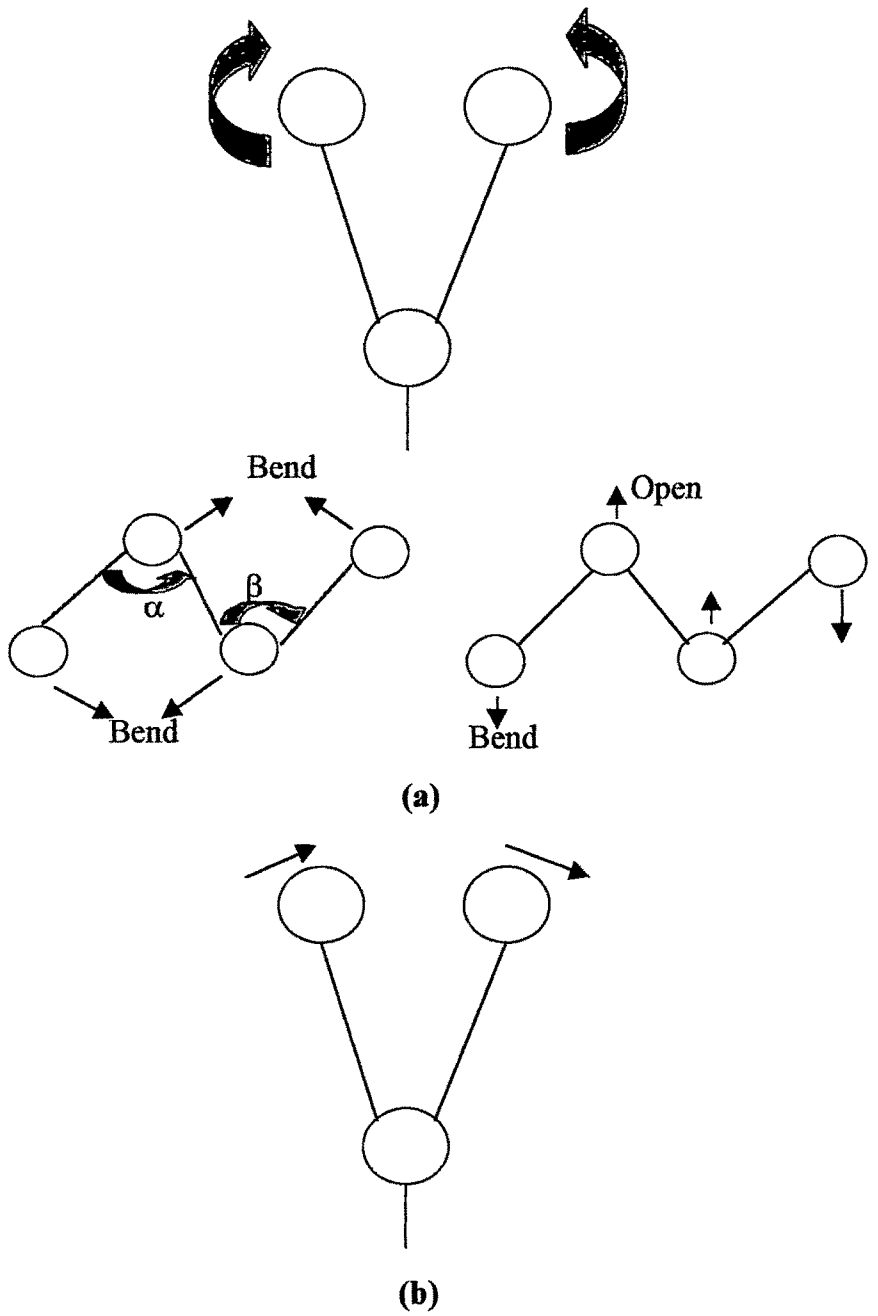

Figure 2.43 : (a) Scissoring Bending (In plane bending with lower frequency of vibration).
(b) Rocking bending ((In plane bending with lower frequency of vibration).

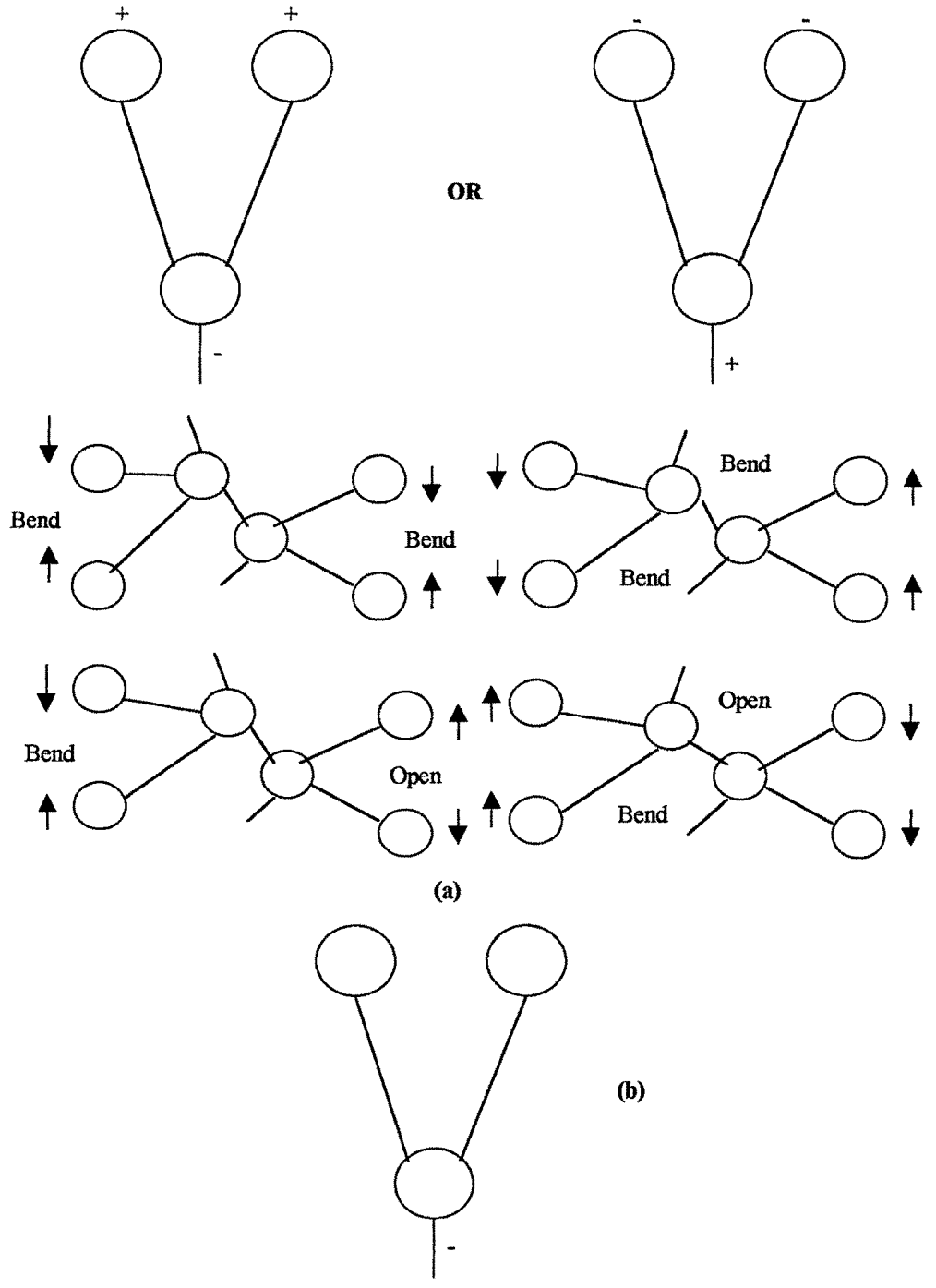

Figure 2.44 : (a) Wagging Bending (Out of plane bending having high frequency of vibration).
(b) Twisting Bending (Out of plane bending with high frequency of vibration).

paper respectively.

Here, the energy required to stretch a spring is more than that needed to bend it so the stretching absorption of a bond will appear at a higher frequency than the bending absorption of a bond. Thus IR spectroscopy is widely used for molecular structural studies of various glasses.

REFERENCE:

1. Colthup. N. B., Daly. L. H. & Wiberley. S. E., "Introduction to Infrared and Raman spectroscopy", 1964, Acad Press, New York & London.
2. H. H. Willard, L. L. Meritt & Jr. J. A. Dean, 'Instrumental Methods of Analysis' Affiliated East-West Press Pvt. Ltd., New Delhi, 4th Eds. 1965, p. 124.
3. Gray. P. & Klein. L. C., J. Non-Cryst. Solids **68**(1984) 75.
4. Sanad. A. M., Kashif. I. F., Sharkawy. A. A. & El Saghier. A. A., J. Mater. Sci. **21**(1986) 3483.
5. Nadjd-Sheibani. R., Hogarth C. A., J. of Mater. Sci. 26(1991)429.
6. C. R. Kurjjain & E. A. Sigety, Phys & Chem of Glass, 9(1968)73.
7. C. R. Kurjjain, J. of Non-Cryst. Solids 3(1970)157.
8. T. K. Bansal & R. G. Mendiratta, Phys. & Chem. Of Glasses, Vol. 28, No. 6(1987)235.
9. T. Nishida & Y. Takashima, J. of Non-Cryst. Solids, 94(1987)229.

2.5 DIFFERENTIAL SCANNING CALORIMETRY (DSC)

2.51 INTRODUCTION:

The thermal method is based on the relationship between temperature and some property of a system such as mass, heat of reaction or volume. Le Chatelier [1] (1887) was the father of thermal analysis. Then other investigator [2-6] studied the thermal changes in a substance during the heat treatment. In a substance, there are mainly two effects occurring the thermal treatment. One is an endothermic effect produced due to a phase transition, dehydration, reduction and some other decomposition reactions. Whereas other is an exothermic effect produced due to crystallization, oxidation and some decomposition reactions. The heat of reaction is proportional to the amount of reacting substance. Therefore various methods which are useful for qualitative identification of substance under investigation and quantitative determination of heat of reaction.

The following are the important method for these investigations[7-8].

(a) Thermogravimetry (TG)

(b) Differential Thermal Analysis (DTA)

(c) Differential Scanning Calorimetry (DSC)

(d) Enthalpimetric Method.

Stone in 1952 [9] developed the first modern, high quality commerical DTA instrument. In 1960s, due to the availability of commercial DTA instrument, this thechnique became an important tool for polymer chemistry. Then after in 1963, the differential scanning calorimetry (DSC) technique came into the existence and stand along with the DTA technique for the elucidation of the thermal properties of properties of polymer.

(a) In differential thermal analysis, the heat absorbed or emitted by a chemical system is observed by measuring the temperature difference between

that system and an innert reference compound [alumina, silicon carbide or glass beads] as the temperature of both are increased at a constant rate[10].

(b) In differential scanning calorimetry, the sample and reference substances are subjected to a continuously increasing temperature; here the heat is added to the sample or to the reference as necessary to maintain the two at identical temperatures i.e., $\Delta T = 0$. The added heat, which is recorded, compensates for that lost or gained as a consequence of endothermic or exothermic reactions occurring in the sample.

In a differential thermal method, the change in the temperature produced due to endothermic or exothermic reaction can be measured. For a given sample temperature T_S and reference temperature, T_R, the difference T_S-T_R is the function recorded [$\Delta T \neq 0$]. The difference of the temperature can be detected by a pair of thermocouples and the generated electromotive force is amplified by appropriate voltage amplification devices. Whereas in DSC, the heat flow is measured as a function of the temperature T with $\Delta T = 0$. The difference between these two techniques ae given in Figure 2.51.

The instruments for these two techniques are of different designs which are as following

(a) Differential Scanning Calorimetry, which are heat flow recording instruments [(dq/dt) $\Delta T = 0$] (Perkin-Elmer, Deltathan & others].

(b) Differential Scanning Calorimetry, which are differential temperature recording " or DTA instruments [$\Delta T \neq 0$] [Dupont, Stone, Fisher, Linsers & others].

The present study has been made using DSC technique and the detailed theory is presented in this chapter.

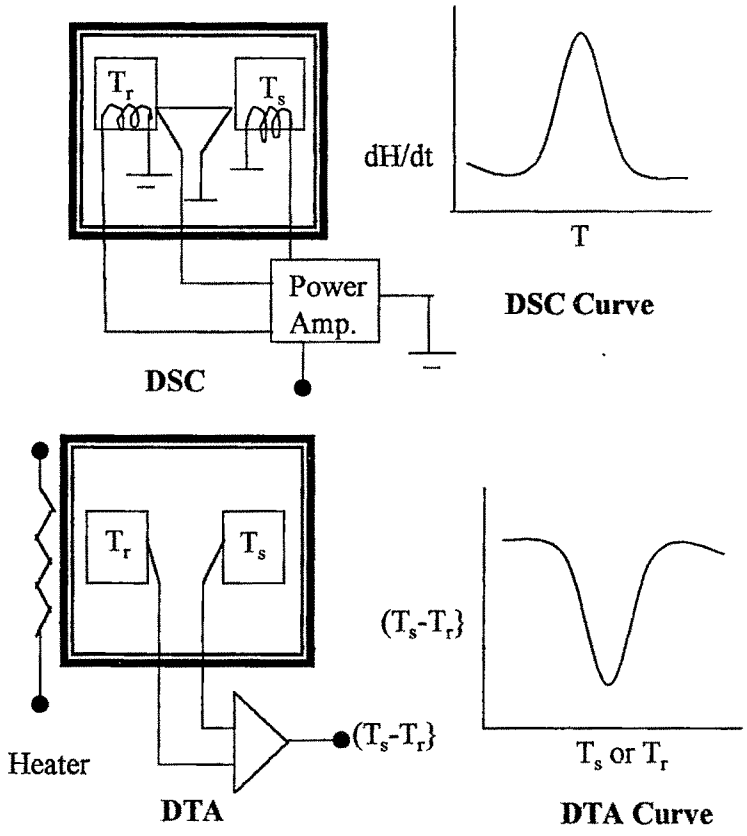

Figure 2.51 : Difference between DSC and DTA technique.

2.52 DIFFERENTIAL SCANNING CALORIMETRY (DSC) TECHNIQUE:

The DSC technique mainly based upon the fact that the sample and reference materials are maintained isothermally [$\Delta T = 0$] to each other by proper application of electrical energy, as they were heated or cooled at a linear rate and the curve is recorded for heat flow dH/dt in mCal/sec as a function of temperature which is shown in Figure 2.52.

An endothermic curve peak is indicated by a peak in downward direction (increase in enthalpy) while exothermic peak is recorded in opposite direction. For a given DSC curve the area enclosed by DSC curve peak is directly proportional to the enthalpy change ΔH_m.

$$\text{Area} = k\,\Delta H_m \qquad (1)$$

Where k is a constant known as calibration coefficient independent of temperature. Using DSC curve in Figure 2.52 a basic equation which relates dH/dt to the measured quantities is given as

$$\frac{dH}{dt} = \frac{-dq}{dt} + \frac{(C_S - C_R)dT_P}{dt} - RC_S\frac{d^2q}{dt^2} \qquad (2)$$

where C_S and C_R are heat capacity of sample and reference holders. R is the thermal resistance. The area under the peak is $\Delta q = -\Delta H$.

A calibration coefficient is still required which is used to convert area to calories and is an electrical conversion factor rather than the thermal constant used in DTA.

The slope of the curve can be described by Newton's law of cooling

$$dq/dt = Ah(T_2 - T_1) \qquad (3)$$

Where h is the interfacial conductivity, A is the area of the interface and T_2-T_1 is the temperature difference between the sample and the holder.

The temperature of the sample T_1 is given by

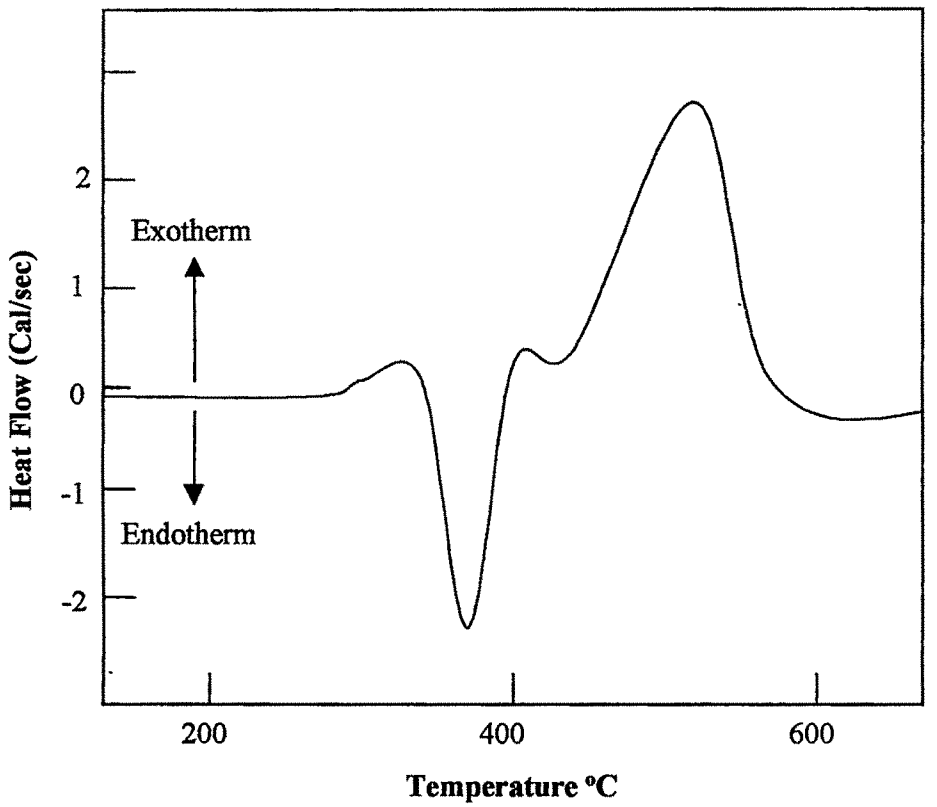

Figure 2.52 : Recommended Presentation of DSC curve

$$T_1 = T_o + \frac{1}{mc}\int \frac{dq}{dt}\,dt \qquad (4)$$

Where T_o is the initial temperature, m is the mass of the sample and c is the heat capacity of the sample.

At a transition, T_2 will remain at the transition temperature T_g for a residence time, t_r determined from

$$\int_0^{t+t_r} \frac{dq}{dt}\,dt = m\,\Delta H_t \qquad (5)$$

Where ΔH_t is the heat of transition. From Equation 5 for a constant heat capacity, the steady slope during the melting transition is

$$\text{slope} = \beta\, hA = k_m\ \beta.c.m \qquad (6)$$

k_m is a decay constant at melting transition, β is a heating rate.

The onset temperature T_i is

$$T_i = T_m + (\beta.c.m/hA) = T_m + \beta/k_m \qquad (7)$$

And the decay constant at the transition is given by

$$K_m = \text{Decay constant} = hA/c.\ M \qquad (8)$$

In DSC curve, it is assumed that the rate of change of the reference material temperature is equal to the programmed temperature.

USES:

(i) The DSC technique is used for determination of the radiation damage of certain polymeric materials, the amount of radiation energy stored in various minerals, heat of adsorption, effectiveness of catalytic materials, heat of polymerization and others.

(ii) Quantitatively, it can be used for the determination of a reactive component in a mixture or the heat of reaction involved in physical and chemical changes.

(iii) This technique finds much use in the qualitative and semiquantitative identification of organic and inorganic compounds, clays, metals, minerals, glasses, fats and oils, polymeric materials, coal and shales, wood and other substances.

(iv) DSC technique is used to determine glass transition temperature, T_g, crystallization temperature, T_c and melting temperature, T_m in glasses. This information is useful for structural study and phase change in glasses.

REFERENCE:

1. Le Chatelier H., Bull. Soc Franc. Mineral 10,203(1987).
2. Ashley. H. F. Ind. Eng. Chem. 3,91(1911).
3. Wholin. R., Sprechsaal 46,749,769,781(1913).
4. Rieke. R., Sprechaal, 44,637(1911).
5. Wallach. H., Compt. Rend, 157,48(1913).
6. Meeler. J. W., & A. D. Holdcraft, Trans. Brit. Cerm. Soc., 10,94(1910-1911).
7. W. W. Wendlandt "Thermal methods of analysis" 2nd ed. P. 172 , Wiley New York , 1974.
8. T. Meisel & K. Seybold, Crit. Rev. Anal. Chem. 12(1981)267.
9. Stone. R. L., J. Amm. Cerm. Soc. 35,76(1952).
10. M. I. Pope & M. D. Judd, Differential Thermal Analysis, Heyden, Philadelphia, 1977.

2.6 THERMOELECTRIC POWER MEASUREMENTS:-

Thermoelectric effects are inevitably associated with flows of heat and electricity. Thermoelectric effects, which are known as Seebeck effect, Peltier effects and Thomson effect are found to be thermodynamically reversible. Microscopic theories describing these effects and based on particular atomic models for the conductor under the treatment given to the *"Thermoelectric Figure of merit"*.

SEEBECK EFFECT:

The Seebeck effect was discovered in 1823 by Thomas J. Seebeck. He found that a current flows in a circuit consisting of two dissimilar metals, when a difference of temperature is maintained between the two junctions. The concentration of electrons at the interface in the two metal is not the same as it depends upon the nature of the metal and its temperature and this results in the transfer of electron from metal of higher electronic concentration to that of lower electronic concentration. This transfer of electrons or charge produces a contact difference of potential across the boundary which neutralizes the effect of the difference in electronic concentration and is responsible for driving the current in the circuit when the temperature of the two junctions is the same, this contact difference of potential is also identical across the two junctions and there is no resultant electromotive force (E.M.F) in the circuit. When, however, one junction is heated relatively to the other, the contact potential at the heated junction becomes more than that at the cold junction and the difference acts as the resultant E.M.F.

For small temperature differences between the junctions, the electromotive force is found to be proportional to the temperature difference and to depend on the nature of the materials comprising the circuit. Referring

to Figure 2.61 (a schematic circuit of two dissimilar conductors, A and B, with junctions at temperature T_o and T) an E.M.F. appears in the circuit such that

$$E_{AB} = S_{AB} AT \qquad (1)$$

Where S_{AB} is defined as relative Seebeck Coefficient between the materials, A and B. E_{AB} and S_{AB} are considered positive if the conventional current tends to flow from A to B at the hot junction.

Since the magnitude of the Seebeck coefficient directly determines the voltage developed by a thermoelectric generator, it would at first appear that the most desirable materials should have the largest Seebeck Coefficients. It has been found that the Seebeck Coefficient of metals range from extremely small values to approximately 80μV/°K. For semiconductor, the range is form 50 μV/°K to 1000μV/°K. The materials specifically developed for thermoelectric applications have Seebeck coefficients approximating 100-400 μV/°K.

Ideally, all the thermoelectric properties should have optimum and invariant values, regardless of the temperature of observation.

The voltage,V, produced between two junction of two dissimilar materials per unit temperature difference between two junctions, ΔT is defined as thermoelectric power, S, of one material relative to another and is a function of the average temperature of the two junction. Thus,

$$S = V/\Delta T \qquad (2)$$

In the Figure 2.62 the thermocouples attached to the specimen are copper-constantan, the thermal e.m.f. in the Cu-sample-Cu circuit and in constantan-sample-constantan circuit give the thermoelectric power of the sample by the following equation-

$$S_{Sample} = \pm\left|\frac{V_{Sample-Cu}}{\Delta T}\right| + S_{Cu} \qquad (3)$$

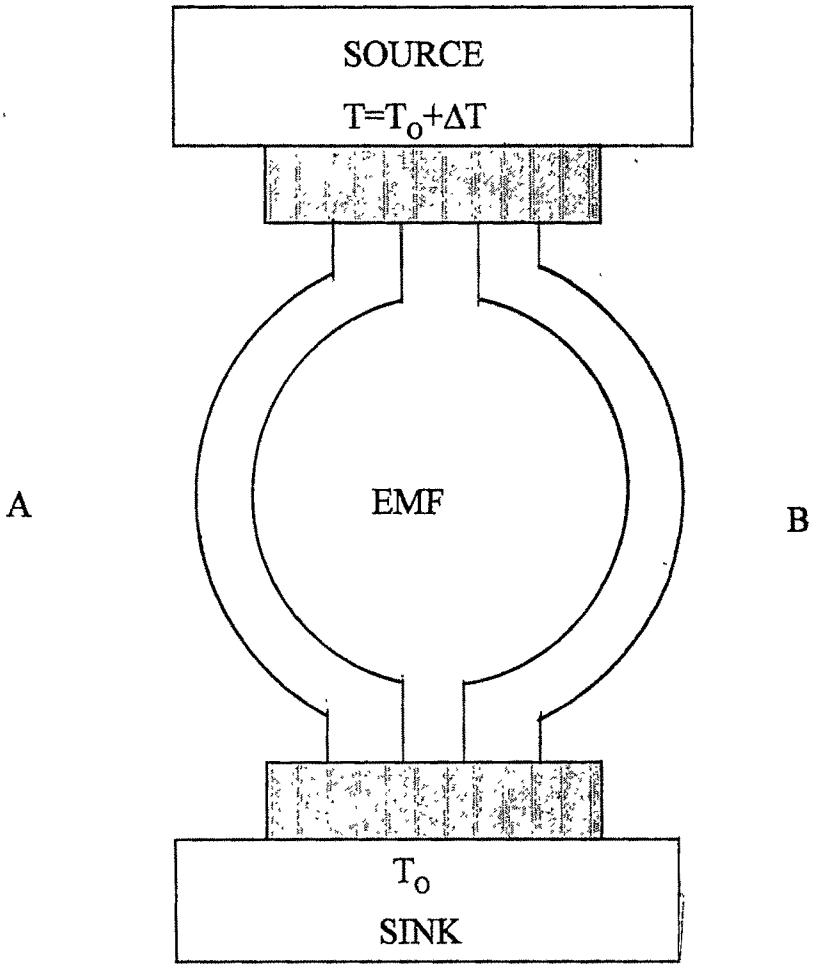

Figure 2.61 : Schematic circuit of Seebeck effect.

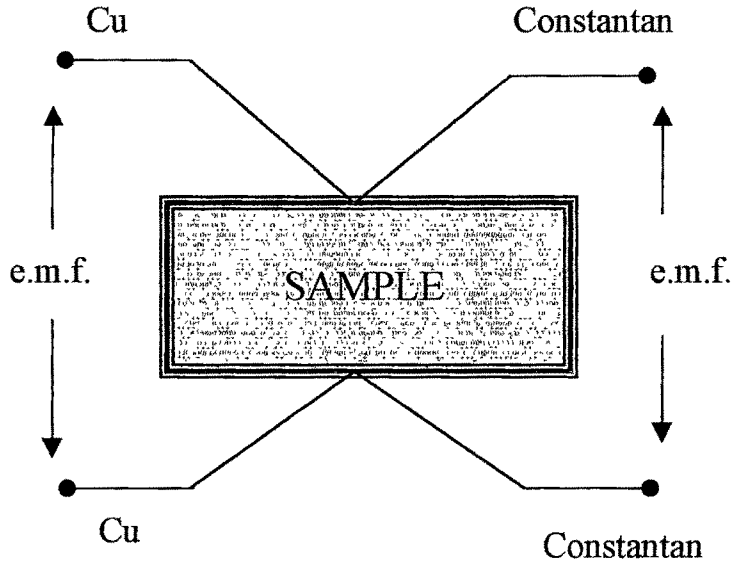

Figure 2.62 : Schematic diagram showing sample and thermocouple of coper-constantan.

$$S_{Sample} = \pm\left|\frac{V_{Sample-Const.}}{\Delta T}\right| + S_{Const.} \qquad (4)$$

where,

S_{sample} is the thermoelectric power of the sample,

$V_{sample\text{-}Cu}$ is the thermal emf of the Cu-sample-Cu circuit,

$V_{sample\text{-}constantan}$ is the thermal emf of the constantan-sample-constantan circuit,

S_{Cu} is the thermoelectric power of copper,

ΔT is the temperature difference between two thermocouples attached to the sample,

S_{const} is the thermoelectric power of constantan.

The negative sign in Equation 3 and 4 is usual for the case $S_{sample} > S_{Cu}$ while positive sign applies whenever $S_{const} > S_{sample}$.

Thermoelectric power, Q, of the glasses found to be dependent on the concentration of transition metal oxide ions (TMO). In V_2O_5 based glasses, the thermoelectric power depends on the ratio of reduced valence ions to total valence ions i.e. V^{+4}/Vt_{otal}. It is well known that V^{+4}/Vt_{otal} ratio is one of the most important factor governing the electrical conduction in glasses containing V_2O_5[1]. The ratio V^{+4}/Vt_{otal} can be determined by the photometric titration using a chemical analysis (Section 3.6)[2]. A mechanism of conduction can be judged by the temperature dependence of the thermoelectric power. A pronounced positive temperature gradient is generally observed for a band semiconductor, while the thermoelectric power, Q, in a hopping semiconductor is nearly independent of temperature. A measurement of thermoelectric power, Q, helps in understanding the nature of semiconductor (oxide glasses) and also gives the important information about a charge carrier whether it is n-type or/p-type. Thermoelectric power of transition metal oxide glasses can be understood by using Heikes and Ure formula[3-4].

$$Q = \left(\frac{k}{e}\right)\left[\ln\frac{C_V}{1-C_V} + \alpha'\right] \quad (5)$$

Where k is a Boltzmann constant, e is the electric charge, C_v is the fraction of low valence state of transition metal ions and constant α' is a constant of proportionality between heat transfer and the kinetic energy of the electrons. It has been suggested by I. G. Austin[5], Appel J.[6] and N. F. Mott[7] that a large polaron hopping conduction can takes place for $\alpha'>>2$, whereas, for $\alpha'<<1$ a hopping conduction is caused by small polarons. This is due to the fact that the small polaron bandwidth (J_p) is very much less than kT [8]. For $\alpha'<<1$, the term α' of the above Equation 5 can be neglected [5] only if the disorder energy, W_D, calculated from $W_D=2(W-W_H)$, with the activation energy W and hopping energy W_H, becomes nearly zero. Therefore, we discussed the conduction mechanism in terms of α' in Heikes formula first by assuming $\alpha'=0$. Calculated value of thermoelectric power, Q_{cal} can be evaluated using Equation 5.

Thermoelectric power, Q, of the semiconducting glasses with TMO is also given by Mackenzie[9-10],

$$Q = \left(\frac{k}{e}\right)\left[\frac{\text{high valence ions}}{\text{low valence ions}}\right] \quad (6)$$

Where, e is the electronic charge of an electron, k is the Boltzmann constant. The ratio $\ln(V^{+5}/V^{+4})$ also helps in understanding the conduction mechanism for these glasses. It has been also discussed that the increase in the concentration of the lower valence state of vanadium (reported V^{+4}) at the expense of V^{+5} rapidly decreases the conductivity of the glasses. With the increase of V^{+5} ions the conductivity of the glasses found to increase[11]. Thus, Mackenzie's formula also helps in understanding the conduction mechanism in glasses.

Reference:

1. J. D. Mackenzie(1964), Modern Aspects of the Vitreous State, Vol. , p. 126., Ed. J. D. Mackenzie, Nutterworth, London.
2. Y. Kawamoto, M. Fukuzuka, Y. Ohta & M. Imani, Phys. Chem. Of Glasses, Vol **20**, No. 3(1979)54.
3. R. R. Heikes, A. A. Maradudin & R. C. Miller, Ann. Phys. NY, **8**(1963)733.
4. R. R. Heikes,"Thermoelectricity" edited by R. R. Heikes and R. W. Ure (Interscience, New York, 1961)p. 81.
5. I. G. Austin & N. F. Mott, Adv. Phys. **18**(1969)41.
6. J. Appel, Solid State Phys. **21**(1968)193.
7. N. F. Mott, Adev. Phys. **16**(1967)49.
8. A. Mansingh & A. Dhawan, J. Phys. C, Solid State Phy. **11**(1978)3439.
9. T. N. Kennedy & J. D. Mackenzie, Phy. & Chem. Glasses **8**(1967)169.
10. T. Allersma & J. D. Mackenzie, J. Chem. Phys. **47**(1967)1406.
11. Janakirama Rao B H V, J. of Amm. Cerm. Soc. **48**, No. 6(1965)311.